Journal of Alloys and Compounds 509 (2011) 4150–4153

Contents lists available at ScienceDirect

Journal of Alloys and Compounds

journal homepage: www.elsevier.com/locate/jallcom

# Effect of Nb doping on the phase transition and optical properties of sol–gel $TiO_2$ thin films

G.Q. Wang[a,b], W. Lan[a,b,*], G.J. Han[b], Y. Wang[b], Q. Su[b], X.Q. Liu[b,*]

[a] Key Laboratory for Magnetism and Magnetic Materials of Ministry of Education, Lanzhou University, Lanzhou 730000, PR China
[b] Department of Physics, School of Physical Science and Technology, Lanzhou University, Lanzhou 730000, PR China

ARTICLE INFO

*Article history:*
Received 4 June 2010
Received in revised form
21 September 2010
Accepted 5 January 2011
Available online 12 January 2011

*Keywords:*
$TiO_2$ thin films
Sol–gel
Phase transition
Nb doping
Optical properties

ABSTRACT

Various content Nb-doped $TiO_2$ thin films were prepared by sol–gel process. XRD analysis shows that the existence of crystalline $TiO_2$ in anatase and rutile form depends on the Nb content in the examined samples. It is observed that Nb promotes the anatase to rutile phase transition but has a depression effect on the anatase grain growth. It is found that incorporation of about 4 at.% of Nb completely transforms anatase $TiO_2$ to the rutile form at a calcination temperature as high as 900 °C. The mechanism is proposed. Optical analyses show that the films have an average of 60% transmission in visible region. The energy gap values using Tauc's formula have also been estimated. The band gap of rutile $Ti_{1-x}Nb_xO_2$ solid solutions increases with increasing $x$.



## 1. Introduction

As a wide band gap semiconductor, titania ($TiO_2$) has been intensively studied due to a variety of potential applications like photocatalysis [1,2], dye sensitized solar cells [3,4], optical fibers [5,6], and gas sensors [7]. One especial area of interest is its photocatalytic activity for environment protection. $TiO_2$ can catalytically decompose a large number of organic and inorganic pollutants like DDT, dichloronitrobenzene, $H_2S$, and NO [8–10]. But for practical application, the photocatalytic activity of $TiO_2$ needs further improvement. The photocatalytic activity of $TiO_2$ has been found heavily depending on its crystal structure. Through the research of the structure and the morphology of a titania photocatalyst (Degussa P25) with multiphase material consisting of anatase and rutile in the approximate proportions 80/20, Bickley and Yu et al. [11,12] found that the photocatalytic activity of $TiO_2$ mixed phase was greater than that of either of the two pure crystalline phases. $TiO_2$ is possessed of three different crystalline forms: anatase (tetragonal), rutile (tetragonal) and brookite (orthorhombic) [13]. The process of the anatase to rutile transformation is affected by many factors, including the synthesis method, the doping element and so on, but the reasons why these different phases are formed is poorly understood. As far as the doping elements are concerned, some metal ions could accelerate the anatase to rutile phase transformation, such as V [14], Ni, Co, Mn, Fe, Cu [15] and Ag [16], and some restrain the phase transformation, for example, Si [17], W [18] and Cr [19]. However, at present the complete mechanism of $TiO_2$ phase transition is still unclear. Further study is needed.

In this work, Nb-doped $TiO_2$ thin films were prepared on quartz glass substrates by sol–gel method. Effects of Nb doping on the phase transition temperature of the films were investigated. The band gap and optical transmission spectra of the films were also investigated.

## 2. Experimental details

The deposition of $TiO_2$ thin films was accomplished by sol–gel technique at ambient temperature. Tetrabutyl titanate and niobium (V) ethoxide were used as precursors and absolute ethanol as a solvent. Acetylacetone (AcAc) was added as a chelating agent to decrease the reactivity and stabilize the sol. Acetic acid was added to initialize hydrolysis by esterification reaction with ethanol. Briefly, a $TiO_2$ sol was prepared by dropping proportional tetrabutyl titanate and AcAc into ethanol. After stirred for 30 min, certain amount of acetic acid was added into the solution. The solution was successively stirred till a clear and transparent sol was obtained. The molar ratios of $n_{\text{acetic acid}}/n_{\text{Ti}}$ and $n_{\text{acac}}/n_{\text{Ti}}$ were optimized to obtain stable sol ($n_{\text{acetic}}/n_{\text{Ti}} = 0.2$ and $n_{\text{acac}}/n_{\text{Ti}} = 0.3$). The Nb doped $TiO_2$ sol was prepared by same procedure as established above. The only difference was the addition of niobium ethoxide solution into the $TiO_2$ sol. The composition of Nb-doped $TiO_2$ sol was as follows: tetrabutyl titanate:niobium ethoxide:AcAc:acetic acid:ethanol = 1:$x$:0.3:0.2:34 in molar rate, where $x$ is the atomic percentage of Nb defined by $x = [\text{Nb}/[\text{Nb} + \text{Ti}]]$. The concentration of Nb was 0, 2, 4, 6 and 8 at.%, respectively. In each case, the sol was aged for about 12 h before coating.

* Corresponding authors. Tel.: +86 931 8912703; fax: +86 8913554.
*E-mail addresses:* lanw@lzu.edu.cn (W. Lan), xqliu@lzu.edu.cn (X.Q. Liu).

0925-8388/$ – see front matter © 2011 Elsevier B.V. All rights reserved.
doi:10.1016/j.jallcom.2011.01.021

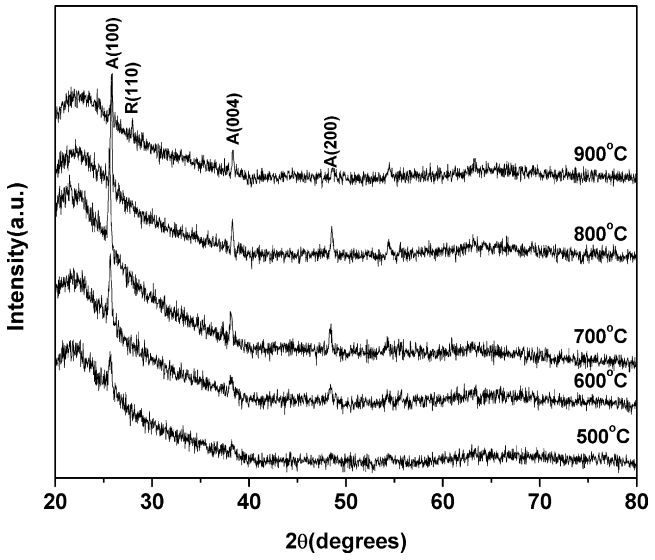


**Fig. 1.** XRD patterns of undoped $TiO_2$ thin films calcined at different temperatures.

$TiO_2$ thin films were prepared by spin-coating onto quartz substrates. Just after coating, the precursor films were dried at 100 °C for 10 min and then 400 °C for 10 min. Finally, dried gel films were calcined at different temperatures for 2 h. The speed rate of heating was 5 °C/min. The corresponding sols were dried to become gels. Subsequently, the gels were used to testing TG–DTA.

The structure and morphology of the films were characterized by X-ray powder diffraction (Rigaku RINT2400 with Cu Kα radiation) and field-emission scanning electron microscopy (Hitach, S-4800), respectively. Thermogravimetric (TG) and differential thermal analysis (DTA) of the gels were carried out in air at the temperature range 20–1000 °C on a PYRIS Diamond TG-DTA High Temp 115 V instrument with a heating rate of 5 °C/min. Spectroscopic analyses of $TiO_2$ films were performed by using a UV–vis spectrophotometer (Tu-1901) in the range of 300–900 nm. The thickness of the films was about 200 nm measured by Surface Profiler.

## 3. Results and discussion

Figs. 1 and 2 show the X-ray diffraction (XRD) spectra of undoped and 8 at.% Nb-doped $TiO_2$ thin films calcined at different temperatures, respectively. Peaks marked 'A' and 'R' correspond to anatase and rutile phases of $TiO_2$, respectively, and the corresponding diffraction planes are given in parenthesis. When the calcined temperature below 900 °C, a well-crystallized anatase form has been found for undoped $TiO_2$ thin films (Fig. 1), which correspond well with the JCPDS data file number 21-1272. While the undoped $TiO_2$ thin films are calcined at 900 °C, a mixture of anatase and rutile phases has been observed with anatase being the predominant one (Fig. 1). For the $TiO_2$ thin film with 8 at.% Nb doped, a completely rutile solid solution is formed with no traces of anatase $TiO_2$ when the calcined temperature is 900 °C (Fig. 2), suggesting that the presence of Nb accelerates anatase to rutile phase transformation. All the peaks observed for this sample correspond to JCPDS data for rutile phase file number 21-1272 (Fig. 2).

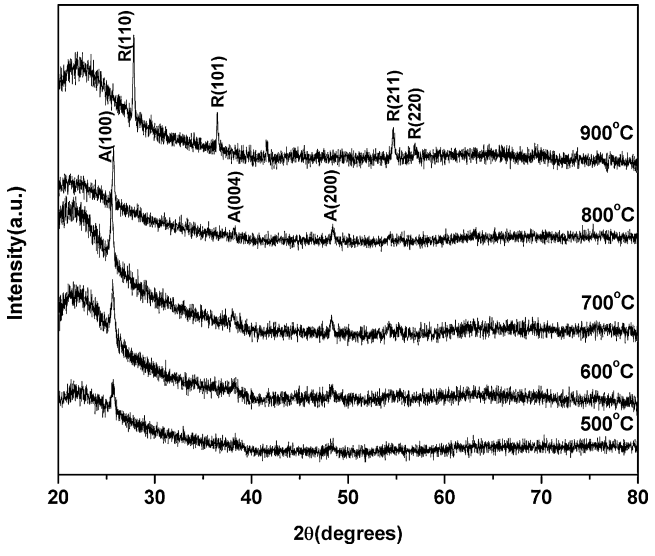


**Fig. 2.** XRD patterns of 8 at.% Nb-doped $TiO_2$ thin films calcined at different temperatures.

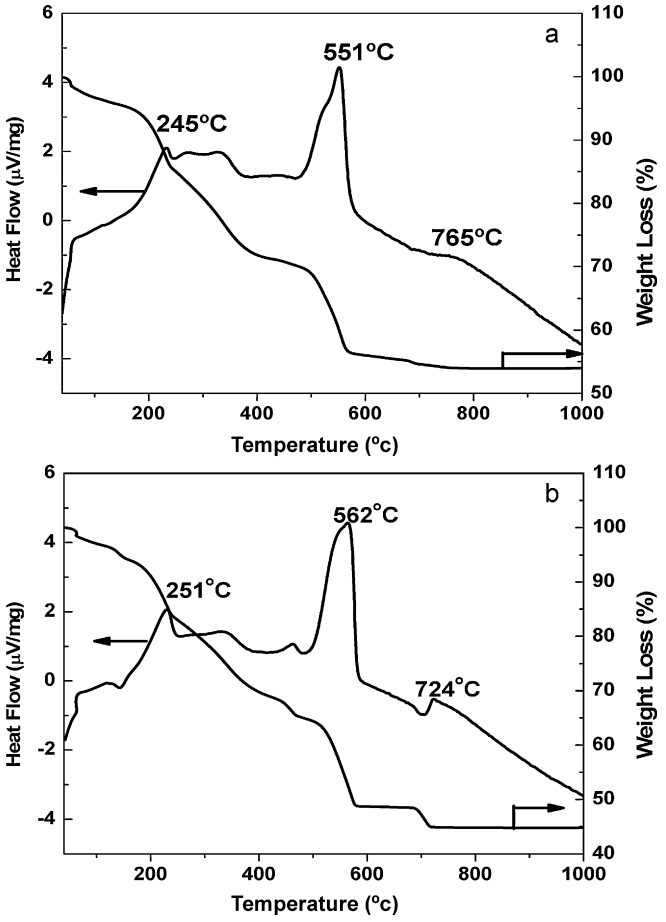


**Fig. 3.** TG and DTA plots for (a) 0 and (b) 8 at.% Nb-doped $TiO_2$ gel powders.

Fig. 3 shows the TG and DTA curves in air for (a) undoped $TiO_2$ and (b) 8 at.% Nb-doped $TiO_2$ gel powders in the temperature range 20–1000 °C. It can be seen that there are several exothermic peaks in the DTA curves. The peaks in the temperature range of 200–500 °C are attributed to the oxidation of some organic substances and $TiO_2$ amorphous to anatase phase transformation [20,21]. Combining with the simultaneous 15–35 wt% lost in the TG traces, the largest exothermal peaks in the temperature region of 500–600 °C might originate from the oxidation of organic groups contained in the $TiO_2$ gel powders and the decomposition of nitrate. The last small exothermic peaks assign to the anatase to rutile phase transition of $TiO_2$ films [16], combining with almost 0 wt% lost in the TG traces. For undoped $TiO_2$ gel powder, the last small exothermic peak assigns at 765 °C to the anatase to rutile phase transition (Fig. 3(a)). Likewise, for 8 at.% Nb-doped sample (Fig. 3(b)), the last peak is observed at a low temperature, i.e. 724 °C, indicating that the presence of Nb decreases the anatase to rutile phase transition temperature. According to the results of XRD and DTA, there is a different phase transition temperature between the film and powder. Different phase transition temperature may be due to the stress

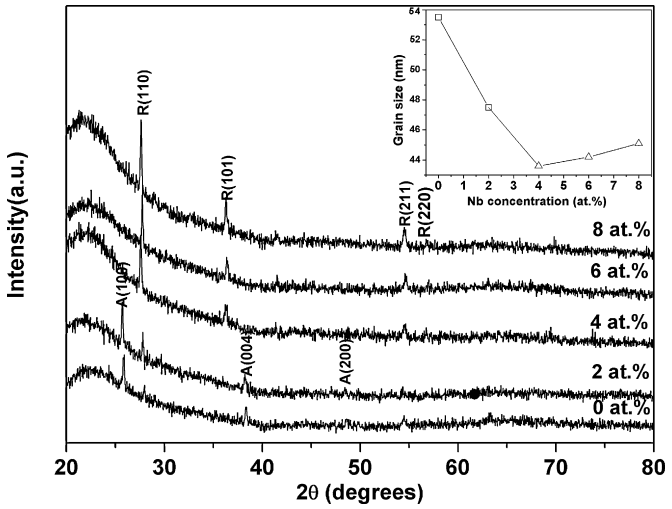


**Fig. 4.** XRD patterns of different concentrations of Nb-doped $TiO_2$ thin films calcined at 900 °C (expressing in atomic percentage; □ average anatase grain sizes, which are determined from the intensity of the anatase (1 0 0) peak; △ average rutile grain sizes, which are determined from the intensity of the rutile (1 1 0) peak).

between film and substrate. The existing of stress in the film delays phase transition temperature compare to that of the powder [22].

For the purpose, investigating the impact of Nb doping content on the phase transition, XRD spectra of $TiO_2$ thin films doped with different amounts of Nb (0, 2, 4, 6 and 8 at.%) annealing at 900 °C are presented in Fig. 4. It is observed that a completely rutile phase is formed until the Nb-doping content is over 4 at.%. The grain size is evaluated using Scherer's equation, and the results are also given in the insert of Fig. 4. A decrease in grain size occurs when samples are loaded with a low percentage of Nb, and then slowly increases as the Nb loading is also increased. It is important to note that the mean grain size of anatase phase decreases and the average rutile grain size increases. The mechanism is discussed below.

The effect of Nb-doped on the $TiO_2$ phase transformation can be attributed to the following facts.

First, as showing in Fig. 4, average anatase grain sizes decrease with the Nb doping, indicating that the Nb dopant has a depression effect on the anatase grain growth. The rutile nucleation and grain growth in those $TiO_2$ films are enhanced. With the anatase grain size decreasing, the total boundary energy for $TiO_2$ thin film increases. The driving force for rutile grain growth then increases and the anatase to rutile phase transition is promoted [23]. Besides, with the anatase grain sizes decreasing, the specific surface area increases and the density of surface defects at the surface of anatase grains would increase. The rutile nucleation is then enhanced occurring at those surface defects and growing towards the bulk. The anatase to rutile phase transformation in the films is promoted.

Secondly, it is well accepted that oxygen vacancies strongly the rate of the rate of the anatase to rutile transformation [24]. When niobium ions enter substitutionally into $TiO_2$, the charge of the $Nb^{5+}$ ions compensated for a decrease in oxygen vacancies. The solubility of Nb in $TiO_2$ depends mainly on temperature and stress. With Nb doping, the concentration of oxygen vacancies at the surface of anatase grains decreases and stress is induced. The solubility of Nb in $TiO_2$ is decreased when temperature is increased. During the calcination process, the uniformly dispersed $Nb^{5+}$ ions would gradually migrate from to the surface of the $TiO_2$ film, because 900 °C is high enough to provide the mobility necessary for our niobium ions to sinter [25]. The solid solubility of Nb in $TiO_2$ is decreased at 900 °C. This would resume the concentration of oxygen vacancies, and the anatase to rutile phase transformation is promoted. The data come from Fig. 4 show an inflexion point at which solid solubility reaches a maximum. This point is found to be around 4 at.% Nb. With 6 at.% and 8 at.% of Nb, the solid solubility of Nb in $TiO_2$ has already exceeded. So this results in more oxygen vacancies, the anatase to rutile phase transformation is enhanced, and grain size of rutile growth bigger.

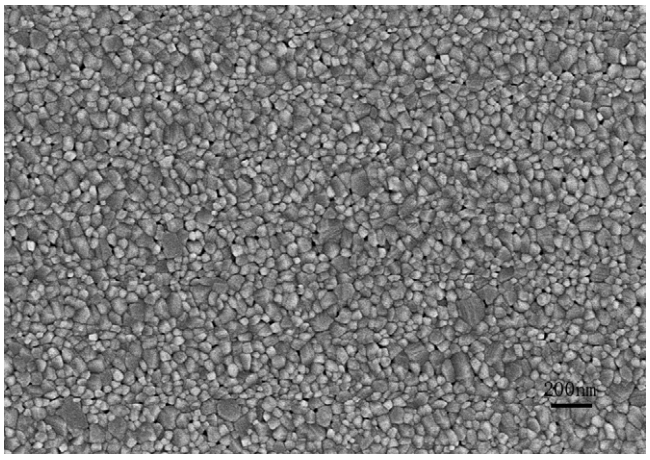


**Fig. 5.** Classical SEM micrographs for undoped $TiO_2$ thin films.

Fig. 5 shows the classical SEM micrographs of an undoped $TiO_2$ thin film. Similar microstructures are observed for Nb-doped films also. As Fig. 5 shows, the surface of the film is dense and smooth. The undoped film shows a granular structure of average size ~50 nm in diameter and occasional large particles appear.

Fig. 6 shows the transmission spectra of undoped and Nb-doped $TiO_2$ films annealing at 900 °C. The transmittance of films is around 60% in visible region. The undoped $TiO_2$ film has high transmittance than Nb-doped $TiO_2$ films. The absorption coefficient values have been computed and found to be in the order of $10^5$ $cm^{-1}$ at the band edge. The optical band gaps have been determined by using Tauc's formula. Fig. 7 shows $(\alpha h\nu)^{1/2}$ vs. $h\nu$ plots for undoped and Nb-doped $TiO_2$ films. The linear nature of the plots above the absorption edge indicates that the fundamental optical transition in $TiO_2$ is indirect. The band gap for undoped $TiO_2$ film is 3.36 eV, which is comparable to the values (3.2–3.3 eV) cited in the literature for anatase $TiO_2$ films [26,27]. The band gap of 8 at.% Nb-doped $TiO_2$ is 3.14 eV. This is comparable to the band gap of rutile (3.0 eV) [28]. Since localized 3d orbitals of Ti constitute the conduction band

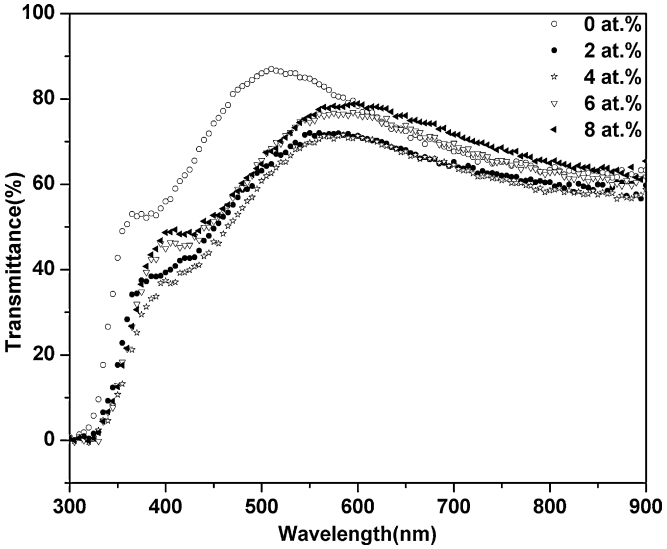


**Fig. 6.** Transmission spectra of Nb-doped $TiO_2$ thin films.

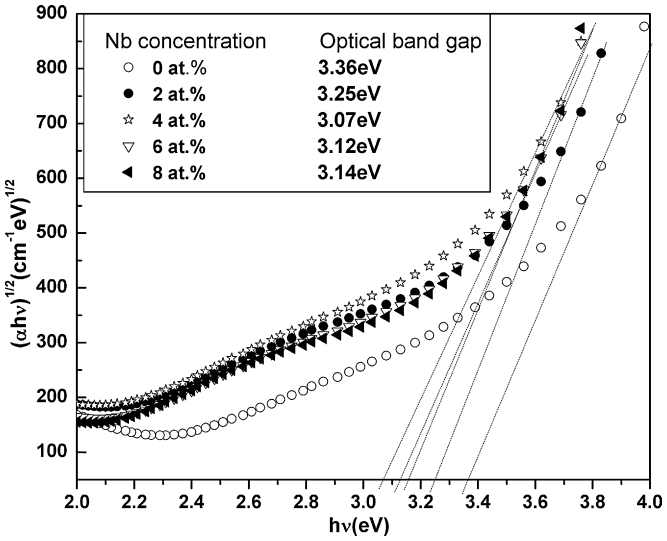


**Fig. 7.** $(\alpha h\nu)^{1/2}$ vs. $h\nu$ plots for Nb-doped $TiO_2$ thin films.

of $TiO_2$, addition of Nb to the $TiO_2$ lattice influences the conduction band by mixing Nb 5s orbitals. Thus, the conduction band is shifted to high energy and a systematic increase in the valence band–conduction band separation with an increasing content of Nb in the $TiO_2$ lattice.

## 4. Conclusions

The undoped and Nb-doped $TiO_2$ thin films prepared by sol–gel method have been studied. It is found that Nb-doped hinders anatase growth and facilitates anatase to rutile phase transformation. For undoped $TiO_2$ thin film, anatase-to-rutile phase transition occurs annealing at 900 °C, and a mixture phase is formed. With the incorporation of about 4 at.% of Nb, complete transformation of anatase to rutile form is observed at 900 °C. Optical analyses show that the films have 60% transmission in visible region. The band gap of rutile $Ti_{1-x}Nb_xO_2$ solid solutions increases with increasing $x$. More work seems to be needed in order to settle the matter of detailed phase transformation mechanisms.

## Acknowledgements

This work was supported by the National Natural Science Foundation of China (Nos. 50802037 and 50872047) and the Fundamental Research Funds for the Central Universities (No. lzujbky-2010-79).

## References

[1] P. Maness, S. Smolinski, D. Blake, Z. Huang, E. Wolfrum, W. Jacoby, Appl. Environ. Microb. 65 (1999) 4094.
[2] J. Wu, X. Lü, L. Zhang, Y. Xia, F. Huang, F. Xu, J. Alloys Compd. 496 (2009) 1–2.
[3] B. O'Regan, M. Gratzel, Nature 353 (1991) 737–740.
[4] L. Zhang, A. Xie, Y. Shen, S. Li, J. Alloys Compd. 505 (2010) 579–583.
[5] A. Danion, J. Disdier, C. Guillard, F. Abdelmalek, N. Jaffrezic-Renault, Appl. Catal. B: Environ. 52 (2004) 213–223.
[6] K. Esquivel, L. Arriaga, F. Rodriguez, L. Martinez, L. Godinez, Water Res. 43 (2009) 3593–3603.
[7] J. Moon, J. Park, S. Lee, T. Zyung, I. Kim, Sens. Actuators B: Chem. 149 (2010) 301–305.
[8] M. Hoffmann, S. Martin, W. Choi, D. Bahnemann, Chem. Rev. 95 (1995) 69–96.
[9] K. Rajeshwar, J. Appl. Electrochem. 25 (1995) 1067–1082.
[10] N. Hamill, L. Weatherley, C. Hardacre, Appl. Catal. B: Environ. 30 (2001) 49–60.
[11] J. Yu, J. Yu, W. Ho, Z. Jiang, New J. Chem. 26 (2002) 607–613.
[12] R. Bickley, T. Gonzalez-Carreno, J. Lees, L. Palmisano, R. Tilley, J. Solid State Chem. Fr. 92 (1991) 178–190.
[13] F. Dachille, P. Simons, R. Roy, Am. Miner. 53 (1968) 1929–1939.
[14] Y. Gao, S. Thevuthasan, D. Mccready, M. Engelhard, J. Cryst. Growth 212 (2000) 178–190.
[15] Y. Iida, S. Ozaki, J. Am. Ceram. Soc. 44 (1961) 120–127.
[16] H. Chao, Y. Yun, H. Xingfang, A. Larbot, J. Eur. Ceram. Soc. 23 (2003) 1457–1464.
[17] K. Okada, N. Yamamoto, Y. Kameshima, A. Yasumori, K. MacKenzie, J. Am. Ceram. Soc. 84 (2001) 1591–1596.
[18] C. Garzella, E. Comini, E. Bontempi, L. Depero, C. Frigeri, G. Sberveglieri, Sens. Actuators B: Chem. 83 (2002) 230–237.
[19] K. Zakrzewska, M. Radecka, M. Rekas, Thin Solid Films 310 (1997) 161–166.
[20] J. Navio, M. Macias, M. Gonzalez-Catalan, A. Justo, J. Mater. Sci. 27 (1992) 3036–3042.
[21] Q. Xu, M.A. Anderson, J. Am. Ceram. Soc. 76 (1993) 2093–2097.
[22] J. Zhang, Z. Yin, M.-S. Zhang, J.F. Scott, Solid State Commun. 118 (2001) 241–246.
[23] G. Oliveri, G. Ramis, G. Busca, V. Escribano, J. Mater. Chem. 3 (1993) 1239–1249.
[24] A. Zielinska, E. Kowalska, J. Sobczak, I. Lacka, M. Gazda, B. Ohtani, J. Hupka, A. Zaleska, Sep. Purif. Technol. 72 (2010) 309–318.
[25] J. Arbiol, J. Cerda, G. Dezanneau, A. Cirera, F. Peiro, A. Cornet, J.R. Morante, J. Appl. Phys. 92 (2002) 853–861.
[26] P. Chrysicopoulou, D. Davazoglou, C. Trapalis, G. Kordas, Thin Solid Films 323 (1998) 188–193.
[27] Z. Wang, U. Helmersson, P.-O. Käll, Thin Solid Films 405 (2002) 50–54.
[28] J. Pascual, J. Camassel, H. Mathieu, Phys. Rev. B 18 (1978) 5606.